or DNA transfer into eukaryotic cells (*25*). The absence of TFSS genes necessary for DNA transfer in the UWE25 genome suggests that in this organism TFSS is responsible for secreting effector proteins into the amoebal host and thus fulfills a function similar to that of the TTSS. The arrangement of UWE25 TFSS genes adjacent to each other in a single region on the chromosome, their higher G+C content (41.9%, 37.9% in the third codon position) compared with the genomic G+C content (35.8%, 26.9% in the third codon position), and the presence of several transposases in proximity to TFSS genes indicates that the TFSS was recently acquired by UWE25 from a donor with a genomic G+C content greater than 42% [estimated according to (*26*)]. The TFSS genes thus represent the only recognized example for a possible recent lateral transfer of genes (coding for proteins with known function) to UWE25 after the split of the chlamydial lineage into its two sister groups.

A recently recognized virulence factor of pathogenic chlamydiae, the protease-like activity factor (CPAF) (*27*), is also encoded in the UWE25 genome (pc0916). CPAF is one of the few proteins that have been shown to be secreted (possibly by means of the TTSS) by pathogenic chlamydiae into the host cytoplasm. Its function is still unknown, but CPAF is able to degrade the human transcription factors required for major histocompatibility complex (MHC) expression (*27*). The presence of CPAF in UWE25, which resides in a host that does not possess a MHC system, indicates that CPAF has evolved from a protease with a different specific function in lower eukaryotic hosts.

Chlamydiae are among the most successful bacterial pathogens of humans and have recently also been associated with chronic diseases (*1*, *9*). Comparative and phylogenetic genome analysis of a chlamydia-related symbiont of amoebae showed that it has retained several key features of the last common chlamydial ancestor and provided evidence that major virulence mechanisms of present-day pathogenic chlamydiae have evolved from the interaction of ancestral chlamydiae with early eukaryotes. Subsequent adaptation of pathogenic chlamydiae to animal and human host cells was most likely mediated by proteins found in modern pathogenic chlamydiae but not detectable by sequence homology in the UWE25 genome (table S3). However, the presence of key virulence factors in environmental chlamydiae, together with their documented ability to multiply in human macrophages (*28*), suggests that these protozoan symbionts have the genetic tools to allow them to infect mammalian cells.

References and Notes

1. J. Schachter, in *Chlamydia*, R. S. Stephens, Ed. (American Society for Microbiology, Washington, DC, 1999), pp. 139–169.
2. W. G. Weisburg, T. P. Hatch, C. R. Woese, *J. Bacteriol.* **167**, 570 (1986).
3. K. D. Everett, R. M. Bush, A. A. Andersen, *Int. J. Syst. Bacteriol.* **49**, 415 (1999).
4. R. Amann *et al.*, *Appl. Environ. Microbiol.* **63**, 115 (1997).
5. T. R. Fritsche *et al.*, *Appl. Environ. Microbiol.* **66**, 2613 (2000).
6. M. Horn *et al.*, *Microbiology* **146**, 1231 (2000).
7. J. M. Ossewaarde, A. Meijer, *Microbiology* **145**, 411 (1999).
8. M. Horn, M. Wagner, *FEMS Microbiol. Lett.* **204**, 71 (2001).
9. M. E. Ward, www.chlamydiae.com.
10. Materials and methods are available as supporting material on *Science* Online. The genome sequence has been deposited at EMBL/GenBank/DDBJ (accession no. BX908798). A comprehensive genome database is available at http://mips.gsf.de/services/genomes/uwe25.
11. R. S. Stephens *et al.*, *Science* **282**, 754 (1998).
12. S. Kalman *et al.*, *Nature Genet.* **21**, 385 (1999).
13. T. D. Read *et al.*, *Nucleic Acids Res.* **28**, 1397 (2000).
14. M. Shirai *et al.*, *Nucleic Acids Res.* **28**, 2311 (2000).
15. T. D. Read *et al.*, *Nucleic Acids Res.* **31**, 2134 (2003).
16. H. Ochman, N. A. Moran, *Science* **292**, 1096 (2001).
17. J. A. Klappenbach, J. M. Dunbar, T. M. Schmidt, *Appl. Environ. Microbiol.* **66**, 1328 (2000).
18. F. S. Brinkman *et al.*, *Genome Res.* **12**, 1159 (2002).
19. G. McClarty, in *Chlamydia*, R. S. Stephens, Ed. (American Society for Microbiology, Washington, DC, 1999), pp. 69–100.
20. R. S. Stephens, in *Chlamydia*, R. S. Stephens, Ed. (American Society for Microbiology, Washington, DC, 1999), pp. 9–27.
21. S. Schmitz-Esser *et al.*, *J. Bacteriol.* **186**, 683 (2004).
22. J. Tjaden *et al.*, *J. Bacteriol.* **181**, 1196 (1999).
23. T. P. Hatch, in *Chlamydia*, R. S. Stephens, Ed. (American Society for Microbiology, Washington, DC, 1999), pp. 29–67.
24. C. J. Hueck, *Microbiol. Mol. Biol. Rev.* **62**, 379 (1998).
25. P. J. Christie, J. P. Vogel, *Trends Microbiol.* **8**, 354 (2000).
26. J. G. Lawrence, H. Ochman, *J. Mol. Evol.* **44**, 383 (1997).
27. G. Zhong, P. Fan, H. Ji, F. Dong, Y. Huang, *J. Exp. Med.* **193**, 935 (2001).
28. G. Greub, J.-L. Mege, D. Raoult, *Infect. Immun.* **71**, 5979 (2003).

29. We thank T. R. Fritsche for arousing our interest in bacterial symbionts of amoebae; W. Goebel, K.-H. Schleifer, A. Leeb, and H. Daims for their support; and M. E. Ward and I. M. Head for critical reading of the manuscript. This work was funded by the bmb+f PathoGenomiK network (grant PTJ-BIO/03U213B).

Supporting Online Material

www.sciencemag.org/cgi/content/full/1096330/DC1
Materials and Methods
SOM Text
Figs. S1 to S9
Tables S1 to S3
References and Notes

2 February 2004; accepted 24 March 2004
Published online 8 April 2004;
10.1126/science.1096330
Include this information when citing this paper.

Protein Displacement by DExH/D "RNA Helicases" Without Duplex Unwinding

Margaret E. Fairman,[1]* Patricia A. Maroney,[2]* Wen Wang,[1] Heath A. Bowers,[1] Paul Gollnick,[3] Timothy W. Nilsen,[2]† Eckhard Jankowsky[1,2]†

Members of the DExH/D superfamily of nucleic acid–activated nucleotide triphosphatases are essential for virtually all aspects of RNA metabolism, including pre–messenger RNA splicing, RNA interference, translation, and nucleocytoplasmic trafficking. Physiological substrates for these enzymes are thought to be regions of double-stranded RNA, because several DExH/D proteins catalyze strand separation in vitro. These "RNA helicases" can also disrupt RNA-protein interactions, but it is unclear whether this activity is coupled to duplex unwinding. Here we demonstrate that two unrelated DExH/D proteins catalyze protein displacement independently of duplex unwinding. Therefore, the essential functions of DExH/D proteins are not confined to RNA duplexes but can be exerted on a wide range of ribonucleoprotein substrates.

DExH/D proteins are required for virtually all phases of RNA metabolism, primarily as essential parts of large ribonucleoprotein (RNP) assemblies, such as the mRNA splicing machinery or viral replication apparatuses (*1*, *2*). It is generally believed that DExH/D proteins couple nucleotide triphosphate (NTP) hydrolysis to conformational changes of such ribonucleoprotein assemblies, which is consistent with the ability of these enzymes to hydrolyze NTPs in a RNA-stimulated fashion in vitro (*1*, *3*). Although it is unknown by which mechanism NTP binding and hydrolysis are used to effect conformational changes in RNP assemblies, it is widely assumed that the biological function of DExH/D proteins involves the NTP-dependent RNA helicase activity that many DExH/D proteins display in vitro, even though physiological targets for almost all DExH/D proteins are not well defined (*4*, *5*).

[1]Department of Biochemistry, [2]The Center for RNA Molecular Biology, School of Medicine, Case Western Reserve University, Cleveland, OH 44106, USA. [3]Department of Biological Sciences, State University of New York at Buffalo, Buffalo, NY 14260, USA.

*These authors contributed equally to this work.
†To whom correspondence should be addressed. E-mail: exj13@po.cwru.edu (E.J.); twn@po.cwru.edu (T.W.N.)

It has recently been demonstrated both in vivo and in vitro that DExH/D enzymes can rearrange RNA-protein complexes (*6*–*8*). Contrary to the traditional assumption that RNA helicase activity is central to DExH/D protein function, some observations made during these experiments suggested that RNP remodeling might not necessarily be coupled to duplex unwinding (*7*–*10*). Because of the central importance of DExH/D proteins in RNA metabolism, it is essential to understand the range of substrates on which these enzymes can act; yet DExH/D "RNA helicases" have never been shown to perform NTP-driven conformational work on RNA or RNPs outside the constraints of RNA secondary structure.

We therefore investigated whether DExH/D proteins could rearrange RNP complexes without duplex unwinding. We chose two model systems in which RNA secondary structure plays no role in protein binding. The first complex is formed between the tryptophan RNA-binding attenuation protein (TRAP) and its specific 53-nucleotide-long cognate RNA (Fig. 1A). No RNA secondary structure surrounds or is contained within the TRAP-binding site (*11*, *12*). TRAP binds to this RNA in a sequence-specific manner as an 11-unit oligomer, and its affinity can be modulated by tryptophan; that is, increasing tryptophan concentrations stabilize the RNA protein complex (*11*).

The second complex is the exon junction complex (EJC) deposited on mRNAs as a consequence of splicing (*13*) (Fig. 1, B and C). Although the exact composition of the EJC remains to be determined, it is composed of at least five distinct proteins that bind tightly in a non–sequence-specific manner approximately 20 nucleotides upstream of exon junctions (*13*, *14*). The EJC plays a variety of roles in postprocessing mRNA metabolism, including nonsense-mediated decay and translational efficiency (*13*, *15*).

We determined whether two distinct DExH/D proteins, NPH-II and DED1, could remodel either or both of the model RNPs. These enzymes were chosen because they are phylogenetically distant within the DExH/D protein superfamily (*16*) and because they differ in distinct and important mechanistic properties. NPH-II is a processive RNA helicase that unwinds duplexes with 3′ single-stranded overhangs (*17*). In contrast, DED1 is nonprocessive (*18*) but unwinds RNA duplexes with single-stranded regions located either 3′ or 5′ to the duplex regions (*19*, *20*).

Two RNAs containing the TRAP-binding site were prepared. One was composed only of the minimal 53-nucleotide TRAP-binding region, whereas the other had a single-stranded, 3′-terminal, 24-nucleotide extension in order to provide a binding site for the DExH/D proteins (Fig. 2, A and B). Both RNAs formed distinct complexes with TRAP that were visualized by nondenaturing polyacrylamide gel electrophoresis (PAGE) (Fig. 2, A and B). TRAP bound to both RNAs with subnanomolar affinity and dissociated with a rate constant k_{off}^{TRAP} of $(2.0 \pm 0.2) \times 10^{-3}$ min^{-1} [in the presence of 10 μM tryptophan (*20*)].

We then assessed the ability of NPH-II and DED1 to disrupt the TRAP-RNA complexes (*21*). NPH-II readily displaced TRAP from the RNA containing the single-stranded extension (Fig. 2A). The displacement was adenosine triphosphate (ATP)–dependent and proceeded with a rate constant $k_{displ}^{TRAP} > 8$ min^{-1} (Fig. 2, C and D). That is, NPH-II accelerated TRAP dissociation by more than three orders of magnitude, indicating that TRAP displacement by NPH-II was an active ATP-driven process. The dislodging of TRAP was not accelerated by NPH-II in the presence of the nonhydrolyzable ATP analog AMPPNP (*20*), indicating that ATP hydrolysis, rather than mere ATP binding, is necessary for active protein displacement. We also observed slight ATP-dependent displacement of TRAP from the RNA lacking the single-stranded extension (Fig. 2B). This result suggested that NPH-II might initiate the reaction either by accessing the exposed backbone of the

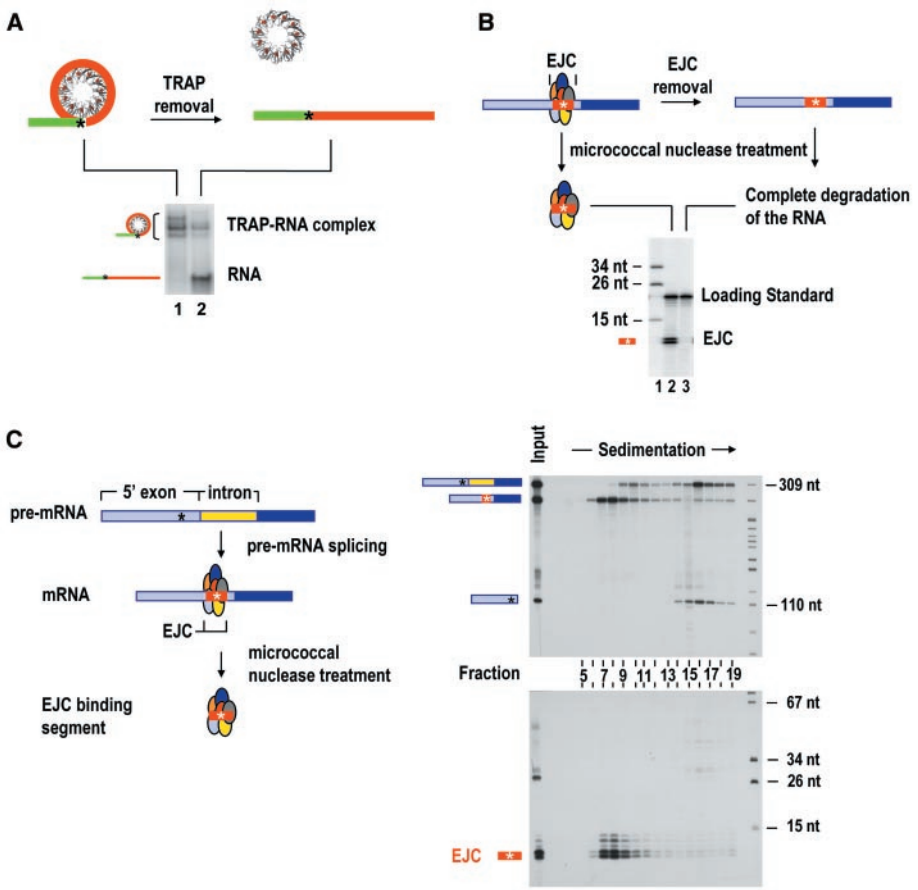

Fig. 1. RNP remodeling without duplex unwinding. (**A**) Remodeling of the TRAP-RNA complex. The radiolabeled RNA contained a 25-nucleotide single-stranded region (green) 3′ to the 53-nucleotide TRAP-binding site (red; radiolabel indicated by asterisk). TRAP binding was visualized by autoradiography of nondenaturing PAGE, resulting in a shift of the labeled RNA (gel panel, lane 1). Upon TRAP removal, free RNA emerged (gel panel, lane 2). The extent of TRAP release was quantified by comparing the amounts of TRAP-RNA to those of free RNA (see methods). (**B**) Displacement of the EJC bound to spliced RNA. A specific radiolabel (asterisk) was introduced into the EJC-binding region (red) (*18*). Removal of the EJC renders the region previously protected from micrococcal nuclease (gel panel, lane 2) susceptible to degradation, which results in the disappearance of the 8- to 10-nucleotide (nt) bands on the denaturing PAGE (gel panel, lane 3). The extent of EJC release was quantified by comparing the amount of EJC-bound RNA in control reactions to that in reactions including DExH/D protein (*18*). (**C**) Partial purification of EJC-containing mRNA. RNA with a specific internal radiolabel was spliced in vitro (*29*), followed by fractionation using glycerol gradient sedimentation. The resulting fractions were analyzed by denaturing PAGE before (right, upper panel) and after (right, lower panel) treatment with micrococcal nuclease (*30*). RNA-bound EJC (characteristic 8- to 10-nucleotide RNA fragments) cofractionated with spliced mRNA.

TRAP-bound RNA or by capturing fraying nucleotides in the TRAP-RNA complex. Nevertheless, the presence of a single-stranded extension significantly increased the displacement efficiency. These results demonstrate that a DExH/D protein can actively remodel a RNA protein complex without any requirement for duplex unwinding.

In sharp contrast to the results obtained with NPH-II, DED1 could not accelerate TRAP dissociation from either RNA under any condition tested (*20*). The failure to actively displace TRAP was not due to compromised DED1 enzyme under the reaction conditions, because DED1 unwound RNA duplexes as expected in control reactions (*20*). Because NPH-II was active in the TRAP displacement reaction and DED1 was not, these experiments also revealed unanticipated selectivity in the function of disparate DExH/D proteins.

To confirm and extend these observations, we then determined whether NPH-II and DED1 could displace the EJC from RNA with single-stranded regions adjacent to the EJC-binding site (Fig. 1B). To assay EJC displacement, pre-mRNA containing a single radiolabeled phosphate at position –21 relative to the 5′ splice site was spliced in vitro (Fig. 1C). In agreement with the results of others (*22*), deposition of the EJC was indicated by the appearance of a specific nuclease-resistant fragment [8 to 10 nucleotides long, centered at –20 on the 5′ exon (Fig. 1C)]. The emergence of the nuclease-resistant RNA fragment was dependent on splicing, and the fragment cofractionated with spliced mRNA during glycerol gradient sedimentation (Fig. 1C). Displacement of the EJC was monitored by loss of nuclease resistance in the EJC-binding region; that is, by the disappearance of the characteristic 8- to 10-nucleotide fragments upon nuclease treatment (Fig. 1B). Although the affinity of the EJC proteins for their binding site cannot be determined directly, EJC dissociation was found to proceed with a rate constant $k_{off}^{EJC} < 10^{-5}$ min^{-1} under the reaction conditions (*20*).

When incubated with DED1 and ATP, we observed a significant decrease in the fraction of bound EJC (Fig. 3A). Negligible displacement was observed without ATP, and significantly less displacement was observed from a "tailless" EJC-RNA complex, prepared by predigestion with nuclease (Fig. 3, A and B). These results indicate that DED1 requires unstructured RNA outside the EJC-binding region to remodel this RNP, although we cannot distinguish whether 5′, 3′, or both overhangs are necessary.

DED1 displaced the EJC from spliced mRNA in a time-dependent manner with a rate constant $k_{displ}^{[DED1]\ EJC} = 0.028 \pm 0.002$ min^{-1} (Fig. 3, C and D). This reflects an at least 3000-fold enhancement over spontaneous dissociation, indicating that DED1 actively displaced the EJC in an ATP-dependent fashion. The rate of EJC displacement was approximately 60 times slower than the unwinding of a control duplex under identical reaction conditions (Fig. 3D), indicating that different processes limit the rates of EJC displacement and duplex unwinding.

We next investigated whether NPH-II was able to displace the EJC. As observed with DED1, a decrease in the fraction of bound EJC was observed in the presence of NPH-II and ATP (Fig. 3E). Only negligible displacement was observed either without ATP or from a tailless EJC-RNA complex (Fig. 3, E and F). This result indicated that NPH-II, too, required single-stranded RNA outside of the EJC to dislodge the EJC in an active ATP-dependent fashion. Like DED1, NPH-II unwound the control duplex faster than it displaced the EJC (Fig. 3H). The lower reaction amplitude observed for EJC remodeling by NPH-II can be tentatively attributed to the depletion of ATP in the reaction mix because of the fast rate at which NPH-II catalyzes ATP hydrolysis (*18*). The nonhydrolyzable ATP analog AMPPNP did not support the reaction with either NPH-II or DED1 (*20*), indicating that ATP hydrolysis was necessary for active EJC displacement.

Despite the lower reaction amplitude with NPH-II, and even though both proteins unwound the control duplex at different rates, NPH-II displaced the EJC with a rate constant highly similar to that observed for

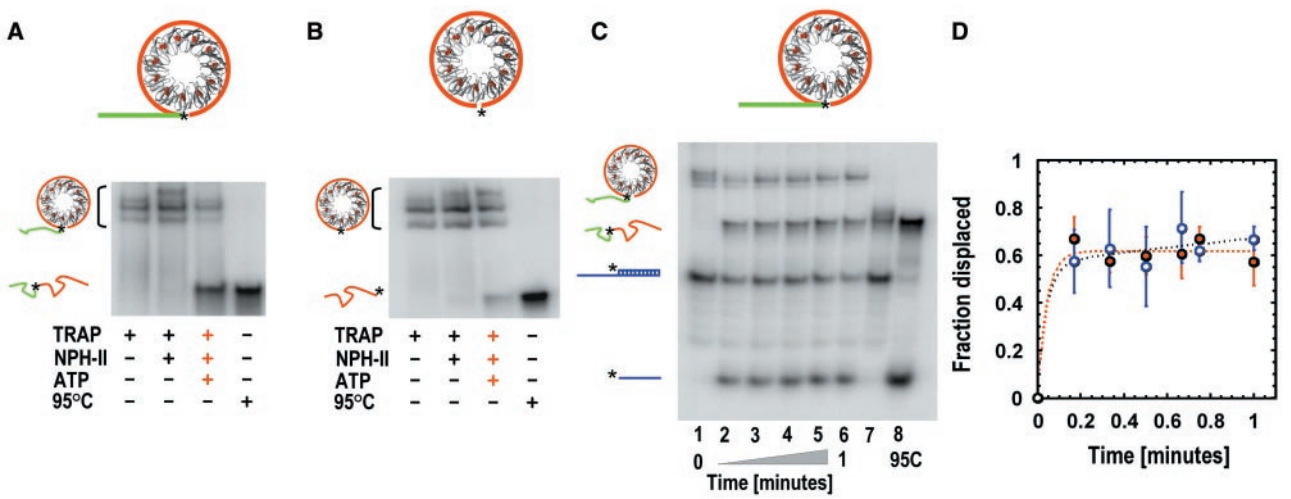

Fig. 2. TRAP displacement from unstructured RNA by NPH-II. (**A**) Displacement of TRAP from RNA containing a single-stranded overhang. Remodeling reactions were stopped after 30 s. TRAP-RNA complexes and free RNA are represented by the cartoons on the left. The apparent heterogeneity of the TRAP-RNA complexes was not due to multiple populations of RNA but was induced by binding of TRAP. (**B**) Displacement of TRAP from the RNA containing only the TRAP-binding site. (**C**) Representative time course for TRAP-RNP remodeling by NPH-II. Reactions with the RNA containing the single-stranded overhang were performed in the presence of a duplex control substrate (16 base pairs containing a 24-nucleotide single-stranded overhang 3′ to the duplex region). Aliquots were removed in 10-s intervals. TRAP-bound RNA, free TRAP substrate RNA, control duplex substrate, and unwound control substrate are indicated by the cartoons on the left. Lanes from left to right are as follows: Lane 1, no ATP added; lanes 2 to 6, time course after ATP addition; lane 7, no TRAP and no NPH-II added; lane 8, sample heated to 95°C for 2 min. The reaction amplitude for TRAP displacement by NPH-II as detected by PAGE constitutes a lower limit for TRAP displacement (*31*). (**D**) Time course for TRAP-RNP remodeling (solid red circles) and simultaneous duplex unwinding (open blue circles). Reactions were repeated multiple times, and data were averaged. Error bars indicate the standard deviation. Reaction rates were too fast to be accurately accessible with the available experimental means; that is, $k_{obs} > 8$ min^{-1}. The apparent amplitude of the duplex unwinding reaction was due to the presence of scavenger DNA (to prevent rebinding of TRAP to the RNA) that partially captures NPH-II during the course of the reaction as well (*17*).

DED1 (Fig. 3, D and H). This raises the possibility that a feature of the EJC, rather than a property of the respective DExH/D protein, dictates the rate of EJC displacement.

Collectively, our data with two different unrelated DExH/D proteins and two different RNP complexes establish that DExH/D proteins can rearrange RNA-protein interactions independently of duplex unwinding, in an active ATP-driven fashion. These results provide evidence that DExH/D proteins can perform ATP-dependent conformational work on RNA that is not based on strand separation. This capability is apparently not restricted to a small subset of DExH/D proteins. In fact, the distant phylogenetic relationship between DED1 and NPH-II within the DExH/D protein family (*16*) renders it rather likely that the capacity to remodel RNA protein complexes independently of duplex unwinding may be a universal property of DExH/D proteins.

The ability of DExH/D proteins to perform ATP-driven conformational work on single-stranded RNA could resemble the movement (tracking) on single-stranded nucleic acids that has been observed for some SF1 DNA helicases; for the termination factor Rho (*23*–*25*); and for the protein MOT1, which dislodges the TATA box–binding protein from DNA (*26*). It is, however, currently unknown whether DExH/D proteins follow single-stranded RNA in an unidirectional and/or processive fashion.

The capacity of DExH/D proteins for ATP-driven conformational work on single-stranded RNA provides a functional explanation for the widely observed stimulation of NTP hydrolysis by single-stranded RNA (*1*). Most important, however, ATP-driven "clearance" of single-stranded RNA might also be the basis for RNA helicase activity by DExH/D proteins, which, in essence, is displacement of a complementary nucleic acid strand from single-stranded RNA (*9*, *10*). ATP-driven conformational work on single-stranded RNA as an underlying mechanism for duplex unwinding would provide a straightforward explanation of the necessity for single-stranded overhangs on the duplexes unwound by most DExH/D RNA helicases (*1*), and it also could explain why certain DExH/D helicases tolerate artificial modifications in only one strand of RNA duplexes (*27*). Although the different rate constants for EJC displacement and duplex unwinding for both DED1 and NPH-II suggest mechanistic differences between duplex unwinding and RNP remodeling, correlations between RNA helicase function and RNP remodeling without duplex unwinding might nonetheless exist. For example, the ability to processively unwind

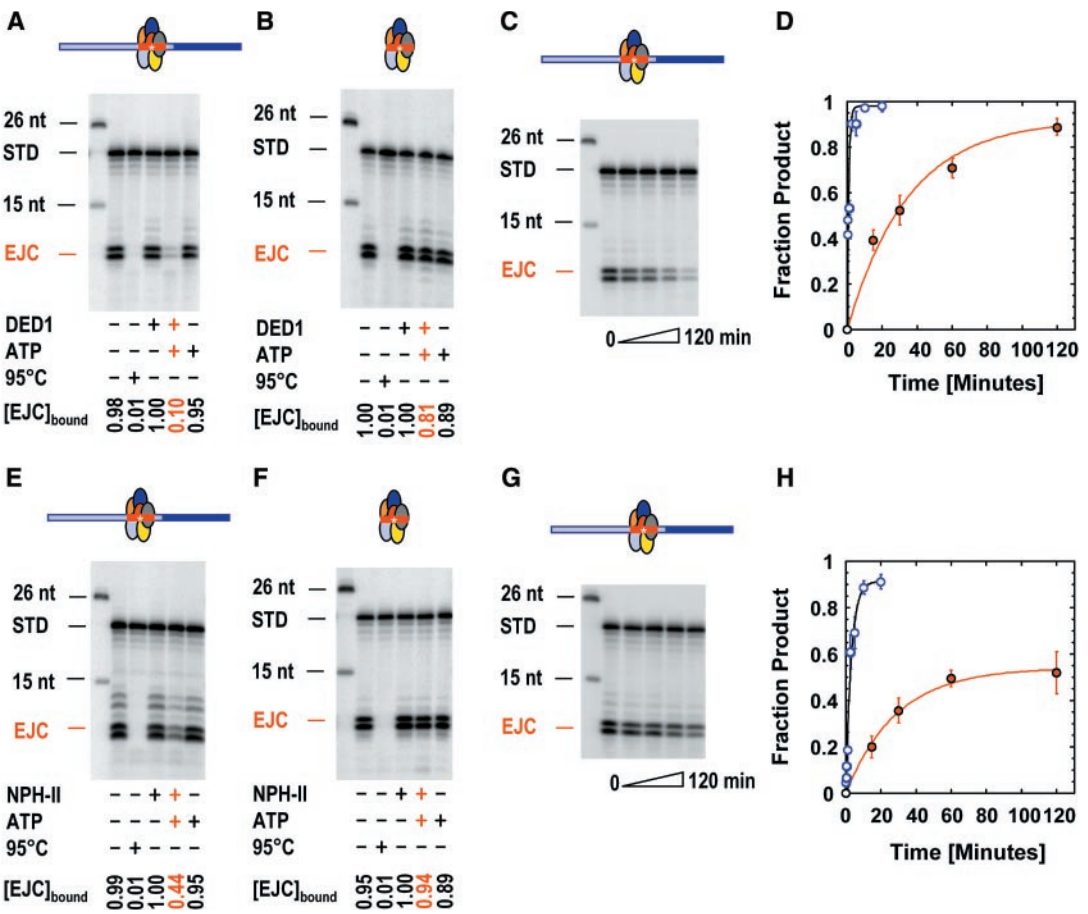

Fig. 3. Displacement of EJC from spliced mRNA. (**A**) DED1-catalyzed EJC displacement from spliced mRNA containing single-stranded overhangs (cartoon). A representative PAGE scan for EJC displacement after 120 min is shown. Labels at left are as follows: EJC, nuclease-protected EJC-binding region, indicating bound EJC (Fig. 1); STD, 22-nucleotide DNA loading standard; 26-nt and 15-nt, size standards. Fractions of bound EJC are indicated underneath the PAGE scan. EJC displacement was measured in multiple reactions, averages are given, and errors ranged from 1% (for bound EJC control) to an average of 14% for the displacement reactions. (**B**) DED1-catalyzed EJC displacement from tailless RNA. Reactions and labels are as described in (A). (**C**) Time course of DED1-catalyzed displacement of EJC from RNA containing overhangs. Aliquots were removed at 15, 30, 60, and 120 min. (**D**) Comparison between reaction rates for EJC displacement (solid red circles) and unwinding of control duplex (open blue circles; substrate was identical to that in Fig. 2C) catalyzed by DED1. Error bars represent the standard deviation calculated from multiple experiments. Unwinding of the control duplex (25-nucleotide single-stranded overhang 3′ to the 16–base pair duplex region) was measured under reaction conditions identical to those for EJC displacement in the presence of partially purified EJC-RNA complex. Unwinding reactions were analyzed and quantified as previously described (*17*). The rate constant for EJC displacement was $k^{[DED1]}_{EJC} = 0.028 \pm 0.002$ min^{-1}. The rate constant for unwinding of the control duplex was $k^{[DED1]}_{unw} = 1.11 \pm 0.14$ min^{-1}. (**E**) NPH-II–catalyzed EJC displacement from RNA containing single-stranded overhangs (cartoon). Reactions and labels are as described in (A). (**F**) NPH-II–catalyzed EJC displacement from tailless RNA. Reactions and labels are as described in (A). (**G**) Time course of NPH-II–catalyzed displacement of EJC from RNA containing overhangs. Aliquots were removed at 15, 30, 60, and 120 min. (**H**) Comparison between reaction rates for EJC displacement (solid red circles) and unwinding of control duplex (open blue circles) catalyzed by NPH-II. Error bars represent the standard deviation from multiple experiments. Unwinding of the control duplex was measured as described in (D). The rate constant for EJC displacement was $k^{[NPH-II]}_{EJC} = 0.032 \pm 0.003$ min^{-1}; the rate constant for unwinding of the control duplex was $k^{[NPH-II]}_{unw} = 0.32 \pm 0.04$ min^{-1}.

RNA duplexes might explain why NPH-II effectively displaces TRAP from its 53-nucleotide-long binding site, whereas DED1, which is not a processive RNA helicase, fails to displace TRAP. For EJC displacement, processive action may not be necessary, because the EJC-binding site comprises only about 10 nucleotides and therefore both DED1 and NPH-II can effectively displace it. Alternatively, because DED1 has been shown to be present in spliceosomal complexes (*28*), displacement of the EJC by DED1 might be potentiated by proteins that co-purify with the EJC preparation but would not be present with the TRAP complex.

The different rates at which NPH-II remodels the TRAP- and the EJC-RNA complexes, and the even starker differences in the rates of TRAP and EJC remodeling observed with DED1, suggest that the properties of a given RNP might also affect the rate at which it can be remodeled by DExH/D proteins. Differences in thermal fraying of nucleotides in the respective protein-binding sites might explain (i) the different rates observed for EJC and TRAP remodeling by NPH-II, (ii) the similarity of rates observed for EJC remodeling with both DED1 and NPH-II, and (iii) the differences between the rate constants for EJC displacement and duplex unwinding. It is thus tempting to speculate that the nature of a given RNP might contribute to the specificity of DExH/D proteins in vivo. Adaptation to the different features of their target RNPs might provide DExH/D proteins with a much greater built-in biochemical specificity toward their biological substrates than was previously concluded on the basis of the largely nonspecific RNA helicase activity of these enzymes.

References and Notes

1. N. K. Tanner, P. Linder, *Mol. Cell* **8**, 251 (2001).
2. G. Kadare, A. L. Haenni, *J. Virol.* **71**, 2583 (1997).
3. J. P. Staley, C. Guthrie, *Cell* **92**, 315 (1998).
4. A. Pause, N. Sonenberg, *Curr. Opin. Struct. Biol.* **3**, 953 (1993).
5. A. Luking, U. Stahl, U. Schmidt, *Crit. Rev. Biochem. Mol. Biol.* **33**, 259 (1998).
6. J. Y. Chen *et al.*, *Mol. Cell* **7**, 227 (2001).
7. A. L. Kistler, C. Guthrie, *Genes Dev.* **15**, 42 (2001).
8. E. Jankowsky, C. H. Gross, S. Shuman, A. M. Pyle, *Science* **291**, 121 (2001).
9. B. Schwer, *Nature Struct. Biol.* **8**, 113 (2001).
10. C. L. Will, R. Luehrmann, *Science* **291**, 1916 (2001).
11. P. Babitzke, P. Gollnick, *J. Bacteriol.* **183**, 5795 (2001).
12. A. A. Antson *et al.*, *Nature* **401**, 235 (1999).
13. H. Le Hir, A. Nott, M. J. Moore, *Trends Biochem. Sci.* **28**, 215 (2003).
14. Removal of all RNA that protrudes from the EJC does not compromise the stability of the EJC (Fig. 3, B and F), indicating that the stability of the EJC-RNA complex does not depend on any RNA secondary structure surrounding the EJC.
15. G. Dreyfuss, V. N. Kim, N. Kataoka, *Nature Rev. Mol. Cell Biol.* **3**, 195 (2002).
16. P. S. Pang, E. Jankowsky, P. Planet, A. M. Pyle, *EMBO J.* **21**, 1168 (2002).
17. E. Jankowsky, C. H. Gross, S. Shuman, A. M. Pyle, *Nature* **403**, 447 (2000).
18. Materials and methods are available on *Science* Online.
19. I. Iost, M. Dreyfus, P. Linder, *J. Biol. Chem.* **274**, 17677 (1999).
20. M. E. Fairman *et al.*, data not shown.
21. TRAP-RNA complexes were formed before the reaction for 10 min. NPH-II was added, and incubation was continued for at least 5 min. Remodeling reactions were started by adding a mixture of ATP and RNA scavenger, which consists of DNA oligonucleotides that hybridize to the TRAP-binding site and thus prevent rebinding of TRAP once it has been displaced. Further materials and methods are available (*18*).
22. H. Le Hir, E. Izaurralde, L. E. Maquat, M. J. Moore, *EMBO J.* **19**, 6860 (2000).
23. K. M. Walstrom, J. M. Dozono, P. H. von Hippel, *Biochemistry* **36**, 7993 (1997).
24. D. E. Kim, M. Narayan, S. S. Patel, *J. Mol. Biol.* **321**, 807 (2002).
25. M. S. Dillingham, D. B. Wigley, M. R. Webb, *Biochemistry* **41**, 643 (2002).
26. R. P. Darst, D. Wang, D. T. Auble, *EMBO J.* **20**, 2028 (2001).
27. T. Hesson, A. Mannarino, M. Cable, *Biochemistry* **39**, 2619 (2000).
28. S. W. Stevens *et al.*, *Mol. Cell* **9**, 31 (2002).
29. P. A. Maroney, C. M. Romfo, T. W. Nilsen, *Mol. Cell* **6**, 317 (2000).
30. P. A. Maroney, C. M. Romfo, T. W. Nilsen, *RNA* **6**, 1905 (2000).
31. NPH-II forms, in an ATP-dependent manner, a tight complex with the RNA from which TRAP has been displaced. This complex could not be disrupted without destruction of the TRAP-RNA complex. The NPH-II–RNA complex co-migrated with the TRAP-RNA complex under all separation conditions tested.

32. We thank P. Linder for kindly providing the DED1 plasmid and S. Shuman for recombinant baculovirus containing the NPH-II expression vector. HeLa Cells were obtained from the National Cell Culture Center. We are grateful to Q. Yang for help with the initial characterization of DED1 and to P. deHaseth and M. Caprara for comments on the manuscript. This work was supported by a grant from NIH to E.J. and by grants from NIH to T.W.N. P.G. was supported by grants from NIH and NSF, and M.E.F. was supported by an NIH training grant.

Supporting Online Material

www.sciencemag.org/cgi/content/full/304/5671/730/DC1
Materials and Methods

13 January 2004; accepted 2 March 2004

Identification of Virus-Encoded MicroRNAs

Sébastien Pfeffer,[1] Mihaela Zavolan,[2] Friedrich A. Grässer,[3] Minchen Chien,[4] James J. Russo,[4] Jingyue Ju,[4] Bino John,[5] Anton J. Enright,[5] Debora Marks,[4] Chris Sander,[5] Thomas Tuschl[1]*

RNA silencing processes are guided by small RNAs that are derived from double-stranded RNA. To probe for function of RNA silencing during infection of human cells by a DNA virus, we recorded the small RNA profile of cells infected by Epstein-Barr virus (EBV). We show that EBV expresses several microRNA (miRNA) genes. Given that miRNAs function in RNA silencing pathways either by targeting messenger RNAs for degradation or by repressing translation, we identified viral regulators of host and/or viral gene expression.

RNA silencing is part of a primitive immune system against viruses in plants (*1*) and insects (*2*). However, its role in viral infection in human cells has not been investigated. EBV is a large DNA virus of the Herpes family that preferentially infects human B cells (*3*). We cloned the small RNAs from a Burkitt's lymphoma cell line latently infected with EBV (*4*). Four percent of the cloned small RNAs originated from EBV (tables S1 and S2). Most of the EBV sequences were cloned more than once, and the analysis of the genomic sequence flanking the cloned RNAs suggested fold-back structures characteristic of miRNA genes (*5*, *6*). The EBV miRNAs originated from five different double-stranded RNA (dsRNA) precursors that are clustered in two regions of the EBV genome (Fig. 1, A and B). The EBV miRNAs were all readily detectable by Northern blotting, including the ~60-nt fold-back precursor for three of the five miRNAs (Fig. 2A). The first miRNA cluster is located within the mRNA of the *BHRF1* (Bam HI fragment H rightward open reading frame 1) gene encoding a distant Bcl-2 homolog (miR-BHRF1-1 to miR-BHRF1-3). miR-BHRF1-1 is located in the 5′ UTR (untranslated region) and miR-BHRF1-2 and -3 are positioned in the 3′ UTR of the *BHRF1* mRNA. The other EBV miRNAs cluster in intronic regions of the *BART* (Bam HI-A region rightward transcript) gene, whose function remains unknown (*7*) (miR-BART1 and miR-BART2).

EBV latently infected cells can be found in three different latent stages (I to III, Fig.

[1]Laboratory of RNA Molecular Biology, The Rockefeller University, 1230 York Avenue, Box 186, New York, NY 10021, USA. [2]Biozentrum der Universität Basel, Klingelbergstrasse 50-70, CH-4056 Basel, Switzerland. [3]Institut für Mikrobiologie und Hygiene, Abteilung Virologie, Haus 47, Universitätskliniken, D-66421 Homburg/Saar, Germany. [4]Columbia Genome Center, Columbia University, 1150 St. Nicholas Avenue, New York, NY 10032, USA. [5]Computational Biology Center, Memorial Sloan-Kettering Cancer Center, 1275 York Avenue, New York, NY 10021, USA.

*To whom correspondence should be addressed. E-mail: ttuschl@rockefeller.edu